

# A Three-Toe Biped Foot with Hall-Effect Sensing

Sergio Castro Gomez, Marsette Vona, and Dimitrios Kanoulas

**Abstract**— This paper describes a novel foot for biped robots designed to provide a reliable and low-cost solution for sensing the Center of Pressure (CoP) on flat and uneven surfaces. The foot uses a new method for detecting contact forces based on measuring the deflection of three flexural toes using Hall-effect magnetic field sensors. We experimentally compare five mathematical models for calculating the CoP coordinates from the sensor data. Results confirm that with the proposed method it is possible to obtain the same level of accuracy and reliability as with standard force sensing resistors, but without some the drawbacks of that approach.

## I. INTRODUCTION

An important aspect of legged robot locomotion is balance. To ensure stability in the walking gait for bipeds most of the current methods rely on the Zero Moment Point (ZMP) criterion. The ZMP is the point on the ground where the component of the moment tangential to the supporting surface, acting on the biped due to gravity and inertia forces, equals zero [2]. The criterion states that during locomotion this point must rely within the convex hull of the foot support points [3], i.e. its support polygon [1]. Falling avoidance is ensured since the robot net forces will always include a counterpart reaction produced by the floor on its feet, generating equilibrium. Thus, it is essential to be able to measure the ZMP accurately.

Summing up the contribution of every link, and using forward dynamics, it is possible to calculate the ZMP. Given that the ZMP is affected by inertias and gravity, the procedure to calculate it involves precise knowledge of the mass, inertia, center of mass, and acceleration of every link of the robot's body. This procedure is not always feasible because of its computational cost and/or the complexity of calibrating and sensing the state of the dynamic model. If the robot is walking on a planar surface it has been shown [2] that the ZMP will always coincide with the Center of Pressure (CoP), which is the location of the resultant force vector equivalent to the field of pressure forces in the soles of the feet of the robot. Furthermore, this equality can be extended to the case of walking on uneven surfaces by defining a virtual surface [2]. This avoids the calculation of the ZMP by measuring the CoP instead. Stable gait can be achieved by using feedback control to ensure that the ZMP will always remain within the support polygon. In order to obtain the CoP, which is based on contact forces acting in

the feet of the robot, some type of force sensor is required, generally located in the foot or ankle.

The main contribution of this work is a new method for sensing the CoP using the deflection of the three toes of a flexural foot. Figure 1 shows the prototype of the 3-toe foot scaled to fit a mini biped robot with approximately the same kinematics as Darwin-OP [12]. More design details are given in Section II. Hall-effect sensors measure the field emitted by magnets in each toe. Force variations on a toe lead to corresponding changes in the position of its magnet, which are detected as changes in the magnetic field. The CoP is calculated as a weighted function of those forces on all three toes. We compare five models for combining these weights (Section III). Experimental results confirm the functionality of the method, which shows the same level of accuracy as Force Sensing Resistor (FSR) sensors, the prior state of the art for low-cost CoP sensing (Section IV). FSRs can be difficult to calibrate, often suffer from drift, and can respond erratically in the presence of off-axis forces which can be hard to avoid [13]. A six-axes load cell installed in the ankle can also measure CoP precisely, but it is about 50 times more expensive. In our experiments we use such load cell for reference.

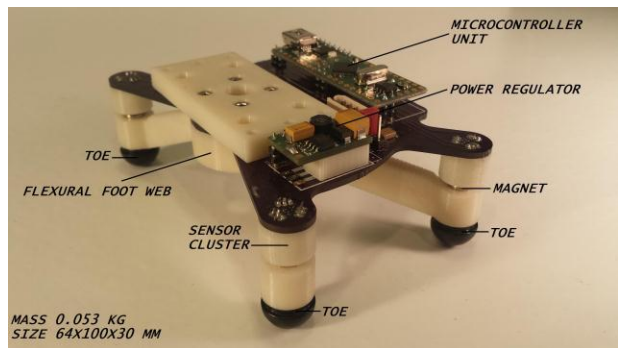


Figure 1. The [64x100x30]mm, 53g, 3-toe foot design. Cost: US \$115.

### A. Related Work

The importance of stability during bipedal locomotion led to the development of several CoP sensing methods [4,7-10]. The sensors that have been used differ in accuracy, size, weight, capability of measuring different variables, and cost.

Universal Force-Moment Sensors (UFS or load cells) have been used widely, e.g. in industry to control the motion of robotic arms in automated processes, to accurately measure the 3 forces and torques applied in the limbs of robots [8]. UFSs are very accurate but because of their dimension and design, most of them are installed in the ankle of the robots which makes the force and torque measurements in the plane of the sole of the foot indirect. Furthermore, their cost is very high (adding commercially available UFS in each ankle would alone cost about US \$15K). The cost of the whole mini-biped robot used in this

\* This material is based upon work supported by the National Science Foundation under Grant No. 1149235.

Dimitrios Kanoulas is with the Department of Advanced Robotics, Istituto Italiano di Tecnologia, Via Morego 30, 16163, Genova. {dimitrios.kanoulas@iit.it}.

Sergio Castro Gomez and Marsette Vona were with Northeastern University, during the development of this work. Boston, MA 02115, USA.

work is about US \$5K in total, while the 3-toe foot prototype costs only US \$115.

Another popular contact force sensor that has been used is the Force Sensing Resistor (FSR), which is a thin polymer film that decreases its impedance when a force is applied. These sensors are usually installed in the sole of the foot to measure reaction forces directly acting from the ground. Because of their convenient price and size, FSRs are used in several legged robots as CoP sensors, particularly for mini-bipeds like Darwin-OP [12]. However, they are incapable of measuring forces acting in axes different than the surface normal and a planar contact area must be ensured in order to obtain a reliable measure. Moreover FSRs may have some repeatability and drift issues, are generally nonlinear, and the level of error when measuring low forces is significantly higher. Despite these constraints, when they are met FSRs can provide acceptable measurements.

Various other approaches have been presented to sense the CoP. In [4], conductive film is used in the sole of the foot to measure the field of forces, while small force sensors installed in special shoes have been used in [8] to record ZMP trajectories of a human walking. In [9] H-slit Beam plates are installed as soles and the CoP is calculated by the level of deformation of the plates.

What happens if the robot is not stepping on flat terrain? One of the requirements for the correct functionality of the FSR sensors is a flat contact area, but flat soles in uneven terrains have a poor contact, decreasing the net area of the support polygon and therefore the range of stability. A more complex type of foot (1.5Kg) has been designed in [10] to deal with uneven surfaces. A system of photo sensors installed in the foot senses information about the unevenness of the ground and the landing foot trajectory is changed to ensure 3 points of contact. The proposed 3-toe foot presents a simpler solution, which provides an acceptable accuracy at lower price, size, and complexity. Since the CoP and the ZMP are equal under the notion of a virtual planar surface [2], both for flat or uneven terrain, our new 3-toe foot has a different geometry and a new CoP measurement method with the intention to maintain an acceptable support polygon area and to ensure correct measurement in uneven surfaces. The use of magnets and Hall-effect sensors gives a low cost and reliable solution, while the size of the sensors and the material of the toes are very light.

## II. 3-TOE FOOT DESIGN

Even robots with vision capabilities, able to find the best footfall locations, will end up dealing with small unevenness on the ground in real-world environments [10]. This “undetectable” unevenness, which could be of the order of centimeters, could be enough to make a robot with flat rigid feet lose stability because of the effect of the unevenness in the shape of the support polygon. For instance if a biped robot steps on a pyramidal unevenness in the floor with its left foot and the point of contact between the pyramid and the sole is located in the center of the foot, this point will be (correctly) measured as the left foot CoP. Performing another step with its right foot under the assumption that its support polygon equals the whole sole of its left foot, while

in reality it is only a single point will obviously bring instability during the stepping.

The solution in [10] was to visually measure uneven ground geometry and try to re-plan the landing of the foot accordingly. Another simpler alternative, instead of changing the motion, could be to try reducing the probability of hitting unevenness while having at least 3 points of contact between the foot and the floor. Three is the minimum number of points required to represent a plane. Clearance between the toes enables contact for a broad range of uneven and curved surfaces. For this reason a 3-toe foot (Figures 1 and 2) has been designed to handle both flat and uneven terrain. To calculate the CoP, measuring the normal forces that are applied on every toe is required. The popular FSR sensors are not a good option in this case, since they require a flat contact surface and perpendicular acting forces.

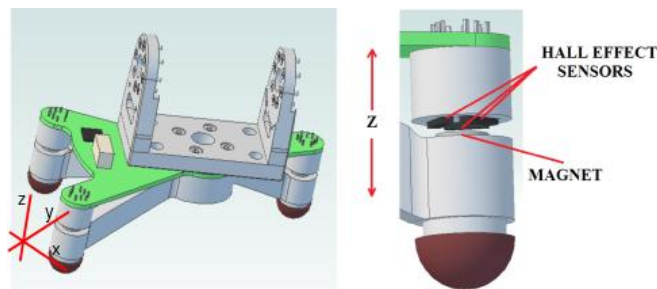


Figure 2. The 3-toe foot (left), and a detailed toe (right).

Instead of measuring the force in the tip of each toe, one could measure the level of deflection of the toes in the presence of force. Even though linearity is not ensured, the level of deflection should monotonically increase with respect to the applied force. The level of deflection could either be measured at the point where each toe is attached to the body of the robot or at the tip of the toe with respect to a reference point. Depending on the material, part of the displacement of the point of contact due to forces could be absorbed across the length of the toe, attenuating the deflection. Therefore, measuring the displacement of the tip of each toe with respect to a reference point would be more appropriate. Figures 1 and 2 show the design of the proposed 3-toe foot, with a circuit board, where the Hall-effect sensors for measuring the deflection of each toe are located (ref points).

With the proposed design 3 points of contact are ensured unless the foot hits any part of the surface that is significantly tall and narrow, which could be avoided by other means. The material and thickness of the foot will determine the level of deflection under a given force and therefore should take into account the biped’s weight. In this prototype, the toes length makes the sensors location coincides with the boundaries of the original Darwin-OP foot. The material is ABS plastic and the toe support dimensions were determined heuristically.

### A. Sensing Toe Deflection based on Magnetic Fields

In order to measure the deflection of the toes, magnets have been installed in them. Variations in the relative position of the magnet with respect to the reference point (in the circuit board) will generate changes in the magnetic field. A set of Hall-effect sensors is installed in the board, forming a triangle. The aim is to measure the position in the  $x,y,z$

direction of each magnet, and then extract the level of force applied over the toe from its relative location. Figure 2 illustrates the details of the magnet and the arrangement of Hall-effect sensors in one of the toes. The z-axis is defined to be parallel to the line that connects the centroids of the (undeflected) magnet and the arrangement of sensors. Variations in the z-axis gap should reflect changes in the level of force normal to the plane of the foot (i.e. the plane of the circuit board and reference points). It could be desirable also to measure changes of the position in other axes as well, since those changes should provide information regarding other forces acting on the foot. For this reason three sensors were used per each toe.

### B. Description of the System Components

The prototype has been integrated with the Geometrical and Physical Computing (GPC) Laboratory biped robot RBPB [14] (Figure 12). This apparatus uses Robotix Dynamixel® servos for controlling the motion of its limbs. The Dynamixel® servos use a communication protocol transported over a serial RS-485 bus. We use a Microcontroller module to implement the foot communication protocol and also to process the information from the Hall-effect sensors. The prototype uses a Crumb644 V1.1 microcontroller module from Chip45. The module includes an Atmega644PA micro controller, 32 I/O ports, and a RS-485 transceiver. The sensors in the prototype are the *Allegro®* A1356 Hall-effect sensors. These are high precision linear sensors with an open drain pulse width modulated (PWM) output.

## III. APPROACHES FOR CALCULATING THE COP

To ensure that the CoP can be calculated on the proposed 3-toe foot, we first need to test the capability of the Hall-effect sensors to measure small changes in the magnet location on each toe. We present a set of test to show that the distance between the sensors and the magnet on each toe can be extracted from the pulse widths measured from its 3 Hall-effect sensors. We then present and compare five mathematical models to obtain the coordinates of the CoP location from the pulse widths perceived from all 9 hall-effect sensors (3 per toe). The internal parameters of all models will be estimated experimentally (Section IV).

### A. Testing the Capability of Measuring Toe Deflection

To test the ability to measure toe deflection we first perform a 1D displacement of the magnets in the z-axis and then a 2D  $xz$ -plane swipe. The relative position of the magnet to the sensors for one toe was controlled using a rigid external positioning apparatus (not shown). The pulse width response of the Hall-effect sensors to the 1D displacement is shown in Figure 3. It is clear that the pulse widths of the signals from the sensors decrease (nonlinearly) with respect to the distance to the magnet in the z-axis direction.

The design of the flexural toe allows deflection in a tangential (x-axis) direction in addition to the normal (z-axis) direction (Figure 2, 3). To confirm that motions along the x-axis can be accommodated, a 2D test was performed. The aim is to obtain a function of the distance between the magnet and the sensors as it moves in the  $xz$ -plane. First, the 2D swipe is performed and the pulse width data are collected

(Figure 4, top). By inverting the pulse widths (Figure 4, bottom) and selecting the maximum one we obtain a function (Figure 5, left) proportional to the real distance in 2D (Figure 5, right).

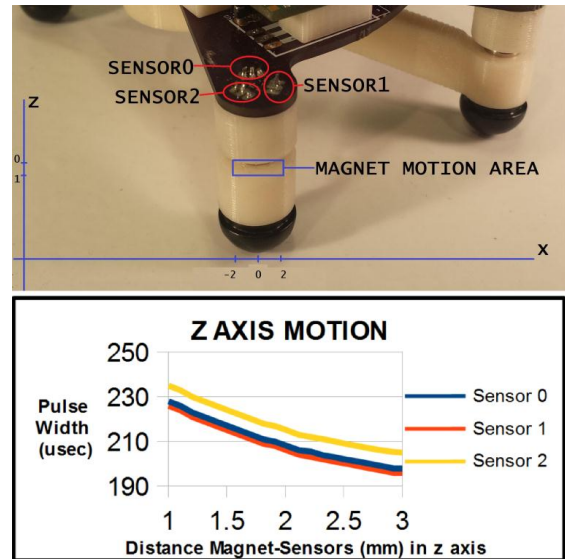


Figure 3. Top: the location of the 3 Hall-effect sensors in each toe, as well as the  $xz$ -plane for the 2D swipe. Bottom: the relation between the sensor's pulse width and the magnet sensors distance in the z-axis.

The results confirm that it is possible to obtain the distance between the sensors and the magnet from the Hall-effect pulse width. It is now required to extract the CoP location from these data.

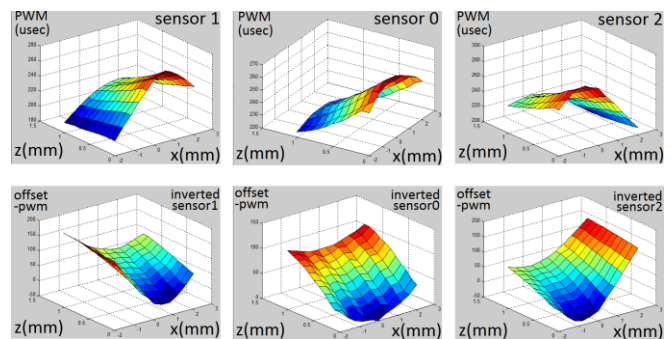


Figure 4. Top: sensor's pulse width response to a 2D swipe of the magnet in one toe. Bottom: the corresponding inverted pulse width.

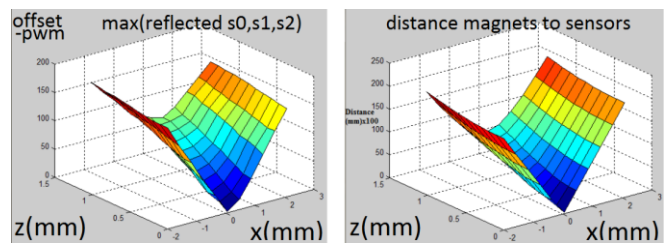


Figure 5. Maximum reflected pulse width (left), and actual distance between the magnet and the sensors in the  $xz$ -plane (right).

### B. Approaches for Obtaining the CoP from Sensor Data

A mathematical model to map pulse widths to the CoP location needs to be determined. The aim is to obtain a 2-

dimensional output  $(x,y)$  that indicates the location of the CoP point  $P$  with respect to a reference point located in the “heel” of the foot. Note that the whole-foot  $xy$  coordinate frame is different from the toe’s  $xz$ -frame defined above. The range for  $x$  will be  $0 \leq x \leq 53$  mm, whereas the range for  $y$  will be  $0 \leq y \leq 88$  mm (Figure 6). Furthermore, the CoP location must lie inside the triangle formed by the centers of the 3 clusters of sensors ( $P0$ ,  $P1$ ,  $P2$ ), which can be expressed as a third constraint  $y \geq 1.66x$ . The inputs of the system ( $S0$  to  $S8$ ) will be the pulse width data from the 9 Hall-effect sensors of the foot. Once the CoP is calculated for each foot, the CoP of the robot will be computed as a weighted average of these when in double support. We compare five different models to calculate the CoP from the magnetic field sensor data.

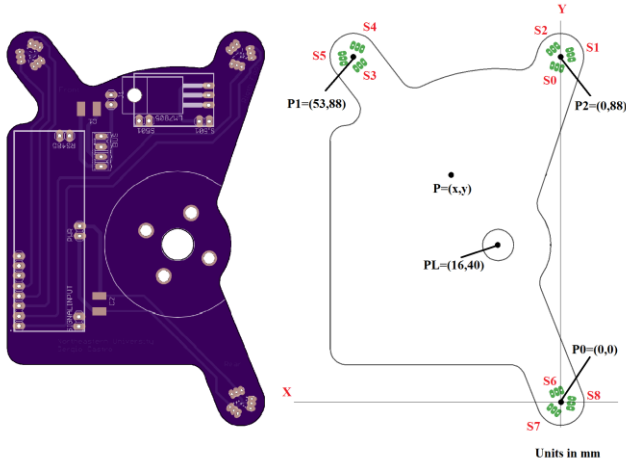


Figure 6. The left foot coordinate system to represent the CoP location  $P=(x,y)$ . The corresponding one for the right foot is a mirror image.

The first approach (*Weighted Average method*, Figure 7), obtains the CoP using the maximum inversed pulse width as input. One way to avoid the inversion is to reinstall the magnet the other way around, generating an opposite polarity in the magnetic field, which is similar to pulse width inversion. This change reduces the input to be the maximum of the sensor’s pulse width per cluster. Yet, the constant of proportionality (denoted as  $w$ ) for each pulse is unknown. This approach consists in finding the values of the weights  $wkx$ ,  $wky$  for  $k=0,1,2$  which correctly converts our pulse widths into the real CoP.  $Cx$  and  $Cy$  are the  $x$  and  $y$  coordinates for each toe. Figure 7 depicts the structure of the function and the unknown variables  $w$ . In other words, the CoP is calculated as the weighted average of the scaled inputs, which are the maximum value of the 3 sensors on each cluster.

Selecting the maximum value may be very sensitive to noise. An alternative method is to compute the mean pulse width of the 3 sensors in each cluster, and use that value as the input to calculate the CoP (*Mean Average method*, Figure 7). The mean acts as a low-pass filter, making the measures less sensitive to noise. Again, the goal is to obtain the value of the scale factors that best reproduces the CoP from the inputs. For both methods the problem has 3 inputs, 6 parameters ( $wkx$  and  $wky$  for  $k=0,1,2$ ), and 2 outputs.

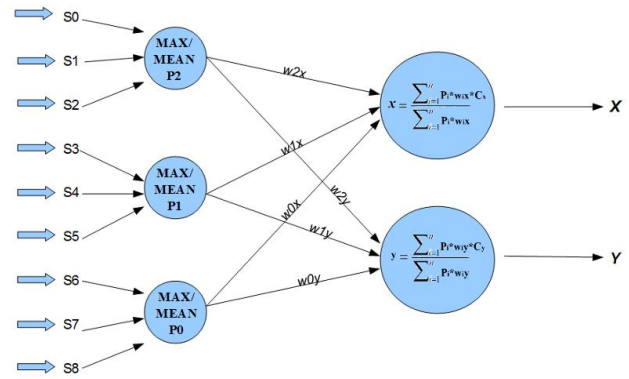


Figure 7. Weighted Average on Maximum (or Mean) pulse width approach to obtain the  $xy$  coordinates of the CoP.

Artificial Neural Networks (ANNs) have shown positive results in fitting linear and nonlinear models, at a low computational cost. In this approach (*ANN method*, Figure 8), no previous knowledge of the system is assumed, and the inputs are not pre-processed. All pulse widths are set as inputs to a single layer ANN, and activation functions deliver the outputs  $x$  and  $y$ . Each pulse width  $S$  is scaled and summed, adding an offset  $b$  to calculate each coordinate. An activation function processes the sum. To simplify the problem, the activation function is set to linear, passing the output of the summation without affecting it. For this method the problem has 9 inputs, 20 parameters ( $bx$ ,  $by$ , and  $wkx$ ,  $wky$  for  $k=0,\dots,8$ ), and 2 outputs.

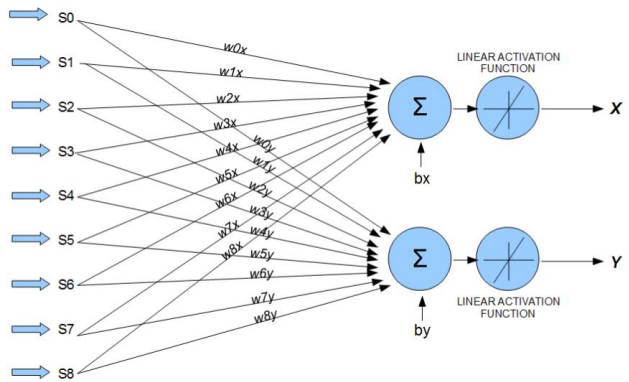


Figure 8. Single layer Artificial Neural Network (ANN) approach to obtain the  $xy$  coordinates of the CoP.

In order to reduce the number of parameters  $w$  in the ANN approach, the number of inputs can be reduced. This can be done by using the average of the inputs per cluster as inputs to a simpler single layer ANN (*Average ANN method*, Figure 9). For this method the number of parameters becomes just 8 ( $bx$ ,  $by$ , and  $wkx$ ,  $wky$  for  $k=0,1,2$ ), instead of the 20 of the previous model.

Finally, a third variation of the ANN approach is presented (*Modified Average ANN method*, Figure 11). In order to add nonlinearity to the model, the squared means of the clusters are included as inputs. Increasing the dimensionality of the data input is frequently used in supervised learning algorithms (support vector machines) to find linear solutions in higher-dimensional spaces to

nonlinear problems. This solution requires 14 parameters and the model has 6 inputs and 2 outputs.

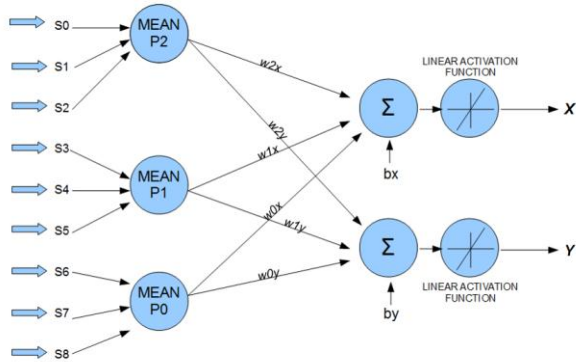


Figure 9. Average Artificial Neural Network (ANN) approach to obtain the  $xy$  coordinates of the CoP.

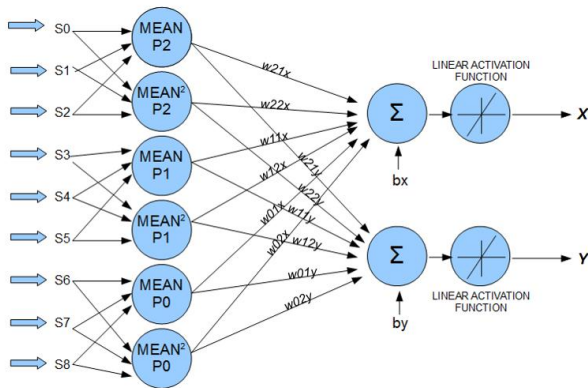


Figure 10. Modified Average Artificial Neural Network (ANN) approach to obtain the  $xy$  coordinates of the CoP.

In all cases, a set of real input-output pairs will be used as training data to estimate the parameters. The inputs will be collected directly from the sensors, whereas the outputs will come from an accurate UFS sensor, which will act as ground truth. We next present the experimental setup, as well as an average error comparison of the proposed approaches with respect to ground truth.

#### IV. TRAINING AND PERFORMANCE OF THE MODELS

We ran a set of experiments to both calculate the weights of the proposed model and validate them. The performance of each model is measured by comparing its output to data from an industrial load cell (UFS) temporarily installed in the robot ankle. The most accurate method is then chosen to obtain the CoP. The experiments also compare the functionality of the system to results with the DarwIn-OP FSR-Embedded sensors.

##### A. Experiment Setup

Input-Output pairs are required to calculate the parameters of the models described in Section III. The 3-toe foot provides pulse widths of the PWM signals from the sensors (inputs). An industrial load cell is used to collect the outputs, which are the  $x$  and  $y$  CoP coordinates. The Rapid Prototyped Biped (RPBP) robot [14] is used to apply forces on the foot, changing the location of the CoP in a defined

sequence. This is accomplished by attaching the robot to a rigid point from the upper side (Figure 12, left) and moving its leg towards the floor, generating an initial load over the foot. Posterior tuning is performed to ensure that the CoP is located in the center of the load cell  $PL$  (Figure 11). A sequence of small position variations of each leg motor is then executed, moving the CoP in all directions. Pulse widths and CoP locations are stored in a table. The experiment was repeated 8 times with 2817 different leg motor variations per trial.

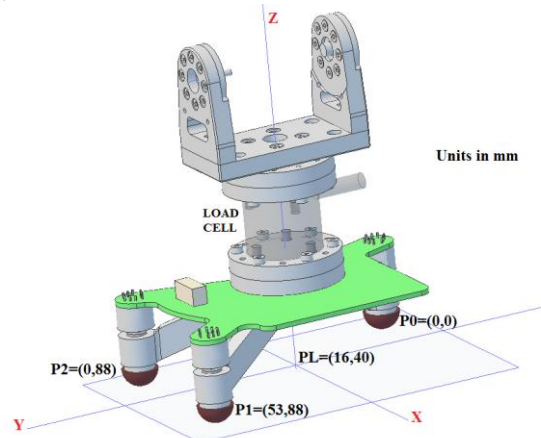


Figure 11. 3-Toe foot assembled to a Load Cell, mounted for running the experiment in the RPBP robot.

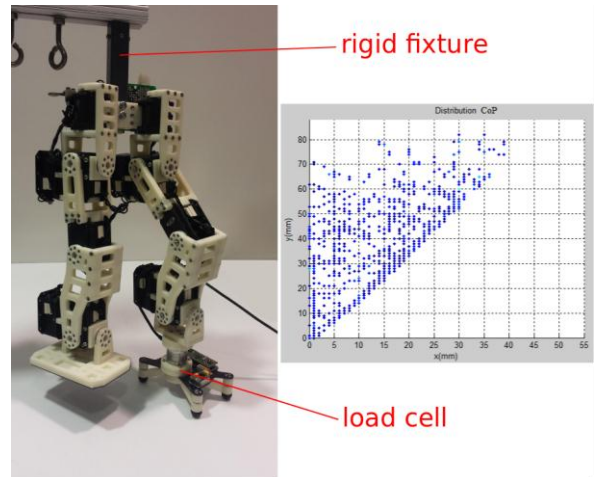


Figure 12. The RPBP robot and the  $xy$  CoP location, measured by the load cell during one trial.

##### B. Errors of the Different Approaches

Using an Evolutionary Algorithm [11] (i.e. a metaheuristic method that iteratively changes the values of the parameters until a minimum error is obtained), the parameters for the 5 models (Figures 7-11, left column of Table 1) were obtained, trying to minimize the squared error with respect to the ground truth provided by the load cell. The dataset of one trial was used to calculate the parameters in all cases. The remaining datasets from the other 7 trials were used to validate the models. The experiment was also executed using the DarwIn-OP FSR-Embedded sensors (bottom row of Table 1). The mean error from the 5 methods, calculated over the 8 datasets, is shown in the right column of Table 1. The average error with respect to the load cell values was calculated when the robot was using the

Darwin foot by running the same experiment 5 times. The average error of the 3-toe foot is of the same order of the DarwIn-OP FSR-Embedded sensors in all cases, and typically less. Even though lower average error is obtained using the weighted average of the maximum pulse width, the weighted average on mean pulse width has been selected to be implemented in the foot given its better behavior in presence of noise.

MEAN ERROR IN MILLIMETERS FOR EXPERIMENTS 1 TO 8									
TECHNIQUE	TEST NUMBER								
	1	2	3	4	5	6	7	8/Average	
Weighted average on maximum pulse width	4.47	3.68	3.91	5.9	2.97	3.26	3.8	3.94	<b>3.99</b>
Weighted average on mean pulse width	5.08	3.71	4.23	5.93	2.79	3.28	3.2	3.83	<b>4.01</b>
Single-layer artificial neural network (ANN)	6	6.73	6.1	8.01	4.8	5.43	4.98	5.85	<b>5.99</b>
Sensor's average ANN	6.3	6.8	6.5	5.4	6.7	5.9	6.1	5.8	<b>6.19</b>
Modified sensor's average ANN	4.64	5.11	4.97	6.37	4.41	4.32	5.01	4.22	<b>4.88</b>
<i>Darwin-OP FSR Foot</i>									<b>6.43</b>

Table 1

### C. 3-Toe Foot Measuring the CoP

The location of the CoP given by the 3-toe foot using the weighted average on mean pulse width, along with the value of the error for each point with respect to the load cell measurement, are shown in Figure 13 for trial 5. Around 90% of the CoP locations given by the 3-toe foot had a difference of less than 6 millimeters with respect to the ground truth. A circle of radius 6 mm corresponds to 4.2% of the support polygon area of the 3-toe foot. The average error when the applied force is at least 16 Newtons (which corresponds to the weight of the robot), is around 2.5 mm. This is because bigger forces produce bigger deflection of the toes, which makes the changes in the magnetic field bigger.

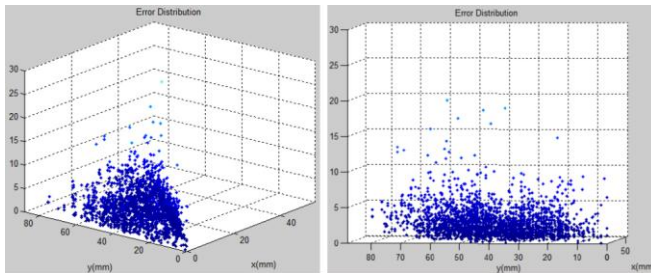


Figure 13. The  $(x,y)$  CoP location and the error distribution (mm) for the 3-toe foot in trial 5 (two views of the same 3D dataset).

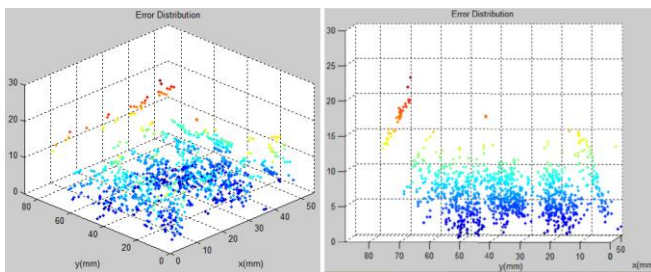


Figure 14. The  $(x,y)$  CoP location and the error distribution (mm) for DarwIn-OP foot in experiment 5 (two views of the same 3D dataset).

The plot of the error distribution for the DarwIn-OP FSR sensor is presented in Figure 14. The area where the CoP can be located in the case of the DarwIn foot is rectangular, following the DarwIn foot geometry. It is also visible that the

FSR sensors have problems calculating the CoP near the edges. In those cases, the contact between the sensors located in the opposite side of the foot and the floor is not good enough to produce a valid measurement. This issue also affects the behavior of the 3-toe foot. From the experiments (Figures 13 and 14) we can see that both the DarwIn sensor and the 3-toe foot present the same level of error.

## V. CONCLUSIONS AND FUTURE WORK

This work presented a novel 3-toe foot design for measuring the CoP. Experimental results demonstrate that the 3-toe foot can be a reliable, low-cost solution sensor for bipeds. Unlike traditional flat feet, the geometry of the proposed foot allows the calculation of the CoP both in flat and uneven surfaces, though testing with the latter is future work. The sensitivity, repeatability, and reliability of the 3-toe foot is comparable to the DarwIn-OP FSR-embedded foot, but its cost is significantly lower. Further analysis of the influence of the geometry (including possibly using 4 or more toes), thickness, and composition of the foot in the sensitivity of the sensing system is required. These design parameters change the mechanical stiffness of the foot, so there is a trade-off between sensing vs ease of control and actuation. Short term future work includes the implementation of stable walking gait algorithms on the RBPB robot using the CoP provided by the 3-toe foot, in both flat and uneven terrain.

## REFERENCES

- [1] K. Erbatur, A. Okazaki, K. Obiya, T. Takahashit, A. Kawamurat. *A Study on the Zero Moment Point Measurement for Biped Walking Robots*. 7th International Workshop on AMC. pp 431 - 436. 2002.
- [2] P. Sardain and G. Bessonnet. *Forces Acting on a Biped Robot. Center of Pressure-Zero Moment Point*. IEEE SMC. pp 630 - 637. 2004.
- [3] M.H.P. Decker. *Zero-Moment Point Method for Stable Biped Walking*. Eindhoven, University of Technology. pp 5. 2009.
- [4] M. Shimojo, T. Araki, A. Ming, M. Ishikawa. *A ZMP Sensor for a Biped Robot*. IEEE ICRA. pp 1200 - 1205. 2006.
- [5] M. B. Popovic, A. Goswami, H. Herr. *Ground Reference Points in Legged Locomotion: Definitions, Biological Trajectories and Control Implications*. Mobile Robots: tow. New Apps. pp 1013 - 1032. 2006.
- [6] D. Krklješ, L. Nagy, M. Nikolić and B. Kalman. *Foot Force Sensor – Error Analysis of the ZMP Position Measurement*. 7th SISY. 2009.
- [7] Q. Li, A. Takanishi and I. Kato. *A Biped Walking Robot Having A ZMP Measurement System Using Universal Force-Moment Sensors*. IEEE/RSJ IROS '91. pp 1568 - 1673. 1991.
- [8] P. Sardain and G. Bessonnet. *Zero Moment Point-Measurements From a Human Walker Wearing Robot Feet as Shoes*. IEEE Trans. on Systems, Man, and Cybernetics. pp 638 - 648. 2004.
- [9] A. Konno, Y. Tanida, K. Abe, and M. Uchiyama. *A Plantar H-slit Force Sensor for Humanoid Robots to Detect the Reaction Forces*. IEEE/RSJ IROS 2005 . pp 4057 - 4062. 2005.
- [10] H. Kang, K. Hashimoto, H. Kondo, K. Hattori, K. Nishikawa, Y. Hama, H. Lim, A. Takanishi, K. Suga, and K. Kato. *Realization of Biped Walking on Uneven Terrain by New Foot Mechanism Capable of Detecting Ground Surface*. IEEE ICRA. pp 5167 - 5172. 2010.
- [11] X. Xie, A. Schneider. *SCO-Social Cognitive Optimization. NLP Solver*. OpenOffice org.
- [12] I. Ha, Y. Tamura, H. Asama, J. Han, D.W. Hong. *Development of Open Humanoid Platform DARwIn-OP*. SICE 2011, pp 2178
- [13] A. Hollinger and M. Wanderley. *Evaluation of Commercial Force-Sensing Resistors*. NIME 2006.
- [14] D. Kanoulas, *Curved Surface Patches for Rough Terrain Perception*. PhD Thesis, Northeastern University, August 2014.